Technical Failure of MR Elastography Examinations of the Liver: Experience from a Large Single-Center Study[1]

Mathilde Wagner, MD, PhD
Idoia Corcuera-Solano, MD
Grace Lo, MD
Steven Esses, MD
Joseph Liao, MD
Cecilia Besa, MD
Nelson Chen, MS
Ginu Abraham, RT
Maggie Fung, MEng
James S. Babb, PhD
Richard L. Ehman, MD
Bachir Taouli, MD

Purpose: To assess the determinants of technical failure of magnetic resonance (MR) elastography of the liver in a large single-center study.

Materials and Methods: This retrospective study was approved by the institutional review board. Seven hundred eighty-one MR elastography examinations performed in 691 consecutive patients (mean age, 58 years; male patients, 434 [62.8%]) in a single center between June 2013 and August 2014 were retrospectively evaluated. MR elastography was performed at 3.0 T (n = 443) or 1.5 T (n = 338) by using a gradient-recalled-echo pulse sequence. MR elastography and anatomic image analysis were performed by two observers. Additional observers measured liver T2* and fat fraction. Technical failure was defined as no pixel value with a confidence index higher than 95% and/or no apparent shear waves imaged. Logistic regression analysis was performed to assess potential predictive factors of technical failure of MR elastography.

Results: The technical failure rate of MR elastography at 1.5 T was 3.5% (12 of 338), while it was higher, 15.3% (68 of 443), at 3.0 T. On the basis of univariate analysis, body mass index, liver iron deposition, massive ascites, use of 3.0 T, presence of cirrhosis, and alcoholic liver disease were all significantly associated with failure of MR elastography ($P < .004$); but on the basis of multivariable analysis, only body mass index, liver iron deposition, massive ascites, and use of 3.0 T were significantly associated with failure of MR elastography ($P < .004$).

Conclusion: The technical failure rate of MR elastography with a gradient-recalled-echo pulse sequence was low at 1.5 T but substantially higher at 3.0 T. Massive ascites, iron deposition, and high body mass index were additional independent factors associated with failure of MR elastography of the liver with a two-dimensional gradient-recalled-echo pulse sequence.

[1] From the Translational and Molecular Imaging Institute (M.W., I.C.S., C.B., N.C., B.T.) and Department of Radiology (I.C.S., G.L., S.E., J.L., C.B., G.A., B.T.), Icahn School of Medicine at Mount Sinai, One Gustave Levy Place, Box 1234, New York, NY 10029; MR Applications and Workflow, GE Healthcare, New York, NY (M.F.); Department of Radiology, New York University Langone Medical Center, New York, NY (J.S.B.); and Department of Radiology, Mayo Clinic, Rochester, Minn (R.L.E.). Received April 13, 2016; revision requested June 6; revision received August 31; accepted September 20; final version accepted October 4. **Address correspondence to** B.T. (e-mail: *bachir.taouli@mountsinai.org*).

Study supported by the National Institutes of Health (1R01DK087877, EB001981). M.W. supported by Société Française de Radiologie.

Diagnosis and staging of liver fibrosis are essential for adequate treatment of patients with chronic liver disease and for assessment of prognosis. Until recently, liver fibrosis was assessed mostly by performing liver biopsy (1), which is invasive and limited by sampling errors (2,3). Multiple noninvasive methods have been developed to decrease the number of liver biopsies at baseline or follow-up.

Transient elastography is an ultrasonographic (US) technique that allows measurement of liver stiffness. Its emergence led to a decrease in the number of biopsies performed for staging of liver fibrosis because of the excellent correlation between liver stiffness measured with transient elastography and liver fibrosis stage, with excellent accuracy for diagnosis of cirrhosis (area under the receiver operating characteristic curve > 0.94) (4). This technique has many advantages, because it is inexpensive, portable, rapidly performed with immediate results, and well accepted by patients. However, transient elastography has several limitations. First, the anatomic extent of the liver is not captured, leading to measurement in a random location. Second, it may be unsuccessful or provide inaccurate measurements in overweight or obese patients and in patients with large-volume ascites. In a large series including 13369 examinations, Castera et al (5) showed that liver stiffness measurements with transient elastography were uninterpretable in nearly 20% of cases, mainly due to obesity (particularly to increased waist circumference) and limited operator experience, with 3.1% failure and 15.8% unreliable results. Other US-based elastography methods have been developed and are used in clinical practice, such as acoustic radiation force imaging (Siemens, Erlangen, Germany) and shear-wave elastography (Aixplorer; Supersonic Imagine, Aix-en-Provence, France). Their main advantages are that they are imbedded in a standard US system, and they allow measurement of liver stiffness with controlled localization. The acoustic radiation-force imaging method has similar performance to that of transient elastography, and shear-wave elastography seems to offer higher performance than does transient elastography for staging of liver fibrosis (6,7). The percentage of uninterpretable results with these techniques was estimated to be 6.7% for acoustic radiation force imaging and 23% for shear-wave elastography (8,9).

Magnetic resonance (MR) elastography is a noninvasive MR imaging method that allows assessment of the viscoelastic or mechanical properties of biologic tissues and provides an estimation of tissue stiffness. Authors of multiple published studies (9–13) have demonstrated that MR elastography is an accurate method that can allow noninvasive detection and stratification of liver fibrosis, with higher performance than that with transient elastography and serum markers and performance similar to that with shear-wave elastography US method. The technical failure rate of MR elastography has been reported in a small number of studies to be approximately 6% (9,14), with no specific report involving high-field-strength (3.0-T) systems. The presence of liver iron has been shown to be responsible for technical failure in most patients; it is present in 71%–100% of cases of technical failure when a two-dimensional gradient-recalled-echo (GRE) pulse sequence is used (9,14). Unlike that of transient elastography, the success of MR elastography does not seem to be influenced by the patient's body mass index (BMI) (14). Authors of these prior studies did not compare the potential factors of failure in successful and failed MR elastography examinations. The aim of our study was to determine the technical failure rate of liver MR elastography at 1.5 T and 3.0 T when a GRE-based pulse sequence is used and to assess predictive factors for liver MR elastography failure in a large single-center study.

Advances in Knowledge

- The technical failure rate of liver MR elastography was higher at 3.0 T than at 1.5 T with the use of a gradient-recalled-echo (GRE) pulse sequence (failure rate, 15.3% [68 of 443] vs 3.5% [12 of 338], respectively; $P < .0001$).
- Iron deposition (failure rate, 25.8% [42 of 163]), massive ascites (failure rate, 56.1% [23 of 41]), and overweight (failure rate, 12.5% [56 of 448]) are predictive factors of liver MR elastography failure.
- The failure rate is higher in the subgroup of patients with advanced chronic liver disease (13.1% [56 of 426]).

Implications for Patient Care

- The higher failure rate with a GRE MR elastography pulse sequence underlines the importance of using alternative pulse sequences at 3.0 T such as the spin-echo echo-planar or fractional GRE pulse sequences.
- In patients suspected of having iron deposition and/or massive ascites, MR elastography should be performed preferably at 1.5 T.

Materials and Methods

Our local institutional review board approved this retrospective single-center,

https://doi.org/10.1148/radiol.2016160863

Content codes: GI MR

Radiology 2017; 284:401–412

Abbreviations

AST = aspartate aminotransferase
BMI = body mass index
CI = confidence interval
EPI = echo planar imaging
GRE = gradient recalled echo
MELD = Model for End-stage Liver Disease
OR = odds ratio

Author contributions:

Guarantors of integrity of entire study, M.W., I.C.S., S.E., G.A., B.T.; study concepts/study design or data acquisition or data analysis/interpretation, all authors; manuscript drafting or manuscript revision for important intellectual content, all authors; approval of final version of submitted manuscript, all authors; agrees to ensure any questions related to the work are appropriately resolved, all authors; literature research, M.W., I.C.S., G.L., S.E., C.B., N.C., R.L.E., B.T.; clinical studies, M.W., I.C.S., G.L., S.E., J.L., C.B., G.A., R.L.E., B.T.; experimental studies, I.C.S., G.L., S.E., G.A.; statistical analysis, M.W., I.C.S., J.S.B., R.L.E.; and manuscript editing, M.W., I.C.S., C.B., M.F., J.S.B., R.L.E., B.T.

Conflicts of interest are listed at the end of this article.

Health Insurance Portability and Accountability Act–compliant study, with a waiver of informed consent.

Patients

Our institutional radiology database was searched to identify consecutive patients who underwent MR elastography of the liver from July 2013 through August 2014 with two of our MR imaging systems equipped with MR elastography capabilities. All MR elastography examinations, both successful and unsuccessful, were included in this convenience sample to compare the frequency of the potential factors for technical failure in those two groups.

The following clinical parameters were recorded for all patients at the time of the MR imaging examination: age, sex, race and ethnicity, weight, and BMI. In patients with chronic liver disease, serum aspartate aminotransferase (AST); serum alanine aminotransferase; serum bilirubin; serum albumin; international normalized ratio; and serum creatinine were recorded, and the AST-to-platelet ratio index and fibrosis-4 scores were computed (15). In patients with cirrhosis (based on MR imaging criteria), the Model for End-stage Liver Disease (MELD) and Child-Pugh scores were also obtained (16,17).

MR Imaging and MR Elastography

All of the MR elastography examinations were performed with either a 1.5-T (GE Signa HDx; GE Healthcare, Milwaukee, Wis; $n = 348$) or 3.0-T (GE Discovery MR750; GE Healthcare; $n = 443$) clinical system by using a 12- and 32-channel body phased-array coil, respectively. Liver MR elastography was performed after administration of a gadolinium contrast agent per clinical protocol (gadoxetic acid, Primovist/Eovist; Bayer Healthcare, Berlin, Germany) (18).

A 19-cm–diameter, 1.5-cm-thick, passive acoustic driver was placed against the right anterior chest wall at the level of the xiphoid process overlying the liver to generate 60-Hz shear waves. Wave imaging was performed by using a modified two-dimensional phase-contrast GRE pulse sequence with motion-encoding gradients along the z-axis and four transverse sections placed through the largest transverse dimension of the liver. The parameters of the pulse sequence were repetition time msec/echo time msec, 48/20; field of view, 30–42 cm (adapted to the patient's body habitus); matrix, 256 × 64; number of signals acquired, one; phase offsets, four; bandwidth, 31.25 kHz; section thickness, 10 mm; array coil spatial sensitivity encoding factor, two. The acquisition time was 55 seconds, split into four breath holds. The stiffness maps were generated automatically by using the multimodel direct inversion algorithm (19,20). For each MR elastography stiffness map, a confidence index map (range, 0%–100%) for stiffness measurement was estimated and automatically provided by the software.

The MR imaging protocol also included the following sequences: transverse and coronal single-shot T2-weighted imaging, transverse fat-suppressed fast spin-echo T2-weighted imaging, transverse three-dimensional T1-weighted imaging in and out of phase, transverse diffusion-weighted imaging, transverse T2* multi–gradient-echo imaging, and transverse three-dimensional T1-weighted breath-hold fat-suppressed spoiled GRE imaging before and after intravenous administration of a gadolinium contrast agent.

Analysis of MR Elastography and Assessment of Failure

Two radiologists (M.W. and I.C.S., with 4 and 1 years of experience in abdominal MR imaging, respectively) independently analyzed the MR elastography examinations. In cases of disagreement, a consensus reading was performed. Technical failure of MR elastography was defined as the absence of visualized wave propagation on the wave images and/or no pixel value with a confidence index higher than 95% on the confidence map (21). The confidence map is a standardized estimate of data quality based on a statistical measure of model fit performance that is provided in all commercial versions of MR elastography.

The quality of the wave propagation was assessed by using a three-point scale: 0, no apparent shear wave imaged or only disorganized wave pattern; 1, poor but sufficient quality; or 2, good quality. The proportion of liver parenchyma covered by pixel values with a confidence index higher than 95% was assessed with a three-point subjective scale: 0, no pixel value; 1, less than 25%; 2, more than 25%. Liver stiffness was measured by one of the observers (M.W.) by using two regions of interest, with a size of 250–350 mm^2, drawn by using the combination of the magnitude images and the confidence map to include liver areas with pixel values with a confidence index higher than 95% and to avoid large vessels and liver edges. The average of the value in the two regions of interest was computed.

Imaging Data Collection

The same two observers also assessed liver morphology (0, normal morphology or noncirrhotic, defined as liver with normal morphology and smooth borders; 1, indeterminate morphology, defined as liver without clear nodular contours, but with some morphologic changes [lobar hypertrophy or atrophy]; and 2, cirrhotic liver, defined as a liver with morphologic changes including enlarged caudate lobe, with nodular contours [with or without signs of portal hypertension]) (22); presence of ascites (0, no ascites; 1, mild, defined as minimal perihepatic or perisplenic fluid; 2, moderate, defined as intraperitoneal fluid without abdominal wall distension; 3, massive, defined as intraperitoneal fluid with abdominal wall distension); and presence of metallic artifacts (from cholecystectomy or prior liver surgery) in the right upper quadrant. Finally, the observers measured the subcutaneous fat thickness at the level of the portal bifurcation and segment 4. The average of the measurements of the two observers was used for analysis.

The liver fat fraction was assessed by using in- and opposed-phase GRE T1-weighted imaging. Two

250–350-mm^2 regions of interest were drawn by three additional observers (G.L., S.E., or J.L., all radiology residents); one was drawn in the right hepatic lobe and one in the left hepatic lobe, avoiding large vessels and any focal liver lesion at the level of the portal bifurcation. The hepatic fat fraction was computed by using the following equation:

$$FF(\%) = SI_{IP} - SI_{OP}/2 \times SI_{IP},$$

where FF is the fat fraction, SI_{IP} is the signal intensity on in-phase images, SI_{OP} is the signal intensity on out-of-phase images. Presence of hepatic steatosis was defined as a fat fraction higher than 5% (23).

Iron deposition was assessed by using region of interest placement similar to that for fat quantification with T2* imaging. Liver T2* maps were automatically provided by the MR imaging system and were computed by using a monoexponential fit of the signal intensity on images from the T2* multi–gradient-echo sequence. Presence of iron deposition was defined as liver T2* less than 24 msec at 1.5 T and less than 14 msec at 3.0 T (24,25).

Statistical Analysis

Results were presented as mean ± standard deviation and range for quantitative variables and number and percentage of patients for categorical variables. Generalized estimating equations based on a binary logistic regression model with a working correlation matrix were used to assess the utility of specific features for the prediction of technical failure of MR elastography. The binary indicator of failure of MR elastography served as the dependent variable and the working correlation matrix was block diagonal with each block representing the covariance matrix for the observations derived for a given subject. Factors significantly associated ($P < .05$) with the outcome were entered in a multivariable logistic model. Patients with missing data were excluded from the multivariable model. Odds ratios (ORs) and their 95% confidence intervals (CIs) were estimated. Since T2* is system dependent, T2* was not considered in multivariable analyses to help in the identification of independent predictors of MR elastography failure; T2* was represented in the multivariable model only through the binary indirect indicator of iron (iron deposition T2* < 24 msec at 1.5 T and < 14 msec at 3.0 T). The significant parameters in the univariate analysis that were only available in the subpopulation with chronic liver disease were not represented in the multivariable model, because we wanted also to include patients without chronic liver disease in the multivariable model. Receiver operating characteristic curve analysis and the Youden index were used to identify a threshold of quantitative parameters (T2*, BMI, weight) that maximized the average of sensitivity and specificity for predicting MR elastography failure. The Cohen κ coefficient for agreement between the two observers for assessment of qualitative MR elastography was calculated to assess interobserver agreement for diagnosis of MR elastography failure. All statistical tests were conducted at the two-sided 5% significance level by using software (SAS 9.3; SAS Institute, Cary, NC).

Results

Patient Characteristics

The cohort included 691 patients (434 [62.8%] were male and 257 [37.2%] were female), with a mean age of 58 years ± 12 (range, 12–86 years). Because some patients underwent repeated MR elastography examinations (one patient underwent four, nine patients underwent three, and 69 patients underwent two examinations), a total of 781 MR elastography examinations were assessed in this study. The indications for liver MR imaging included chronic liver disease in 650 (83.2%) examinations, focal liver lesions in 92 (11.8%) examinations, elevated liver enzymes in 19 (2.4%) examinations, and other indications in 20 (2.6%) examinations. The etiology of liver disease is detailed in Table 1.

MR Imaging and MR Elastography Data

Among the 781 MR imaging examinations, 338 (43.3%) were performed at 1.5 T and 443 (56.7%) were performed at 3.0 T. Liver morphology was normal in 253 (32.4%), indeterminate in 102 (13.1%), and cirrhotic in 426 (54.5%) examinations. The fat fraction was available in 778 (99.6%) examinations. The average calculated fat fraction was 3.4% ± 5.8 (range, −14% to 39%), with 233 (29.8%) examinations showing liver steatosis (fat fraction ≥ 5%). T2* was available in 767 (98.2%) MR imaging examinations. The average T2* was 26.6 msec ± 6.8 (range, 4.7–43.4 msec) at 1.5 T and 19.9 msec ± 6.7 (range, 4.5–58.6 msec) at 3.0 T, with 163 of 781 (20.9%) examinations demonstrating iron deposition (89 at 1.5 T and 74 at 3.0 T). A metallic-related artifact was observed in 236 of 781 (30.2%) examinations. The mean subcutaneous fat thickness was 12.5 mm ± 6.2 (2.0–47.5 mm). Ascites was present in 230 (29.4%) examinations, including 41 (5.2%) with massive ascites.

Technical failure of MR elastography was observed in 12 of 338 (3.5%) examinations at 1.5 T and 68 of 443 (15.3%) examinations at 3.0 T, for a total of 80 (10.2%) examinations with technical failure. In total, there were 55 (7.0%) instances of no wave propagation or only disorganized wave pattern and 25 (3.2%) instances with presence of waves but no liver coverage on the confidence map.

There was excellent interobserver agreement for assessment of MR elastography failure (Cohen κ coefficient, 0.781). In the 701 technically successful MR elastography examinations, mean liver stiffness was 5.1 kPa ± 3.0 (range, 1.2–17.6 kPa). The waves had poor but sufficient penetration in 69 (9.8%) examinations and good penetration in 632 (90.2%) examinations. The coverage on the confidence map was lower than 25% of the liver parenchyma in 95 (13.6%) examinations and larger than 25% of the liver in 606 (86.4%) examinations.

Table 1

Characteristics of the Study Population

Characteristic	Data
Total study population	691
Age (y)	58 ± 12 (12–86)
Sex	
Male	434 (63)
Female	257 (37)
Weight (kg)*	76.7 ± 15.7 (38–139)
BMI (kg/m^2)*	26.8 ± 4.8 (14–47)
BMI category	
<19	16 (2)
19–25	220 (32)
25–30	263 (38)
> 30	142 (21)
Not available	50 (7)
Race	
White	202 (29)
Nonwhite	288 (42)
Unspecified	201 (29)
Chronic liver disease	567 (82)
Subpopulation with chronic liver disease	567
Cause of chronic liver disease	
Hepatitis C virus	299 (53)
Hepatitis B virus	106 (19)
Alcohol abuse	47 (8)
Nonalcoholic steatohepatitis	49 (9)
Other	53 (9)
Miscellaneous (association of multiple causes)	13 (2)
AST (U/L)*	66.5 ± 66.4 (10–928)†
Alanine aminotransferase, (U/L)*	59.7 ± 70.4 (5–931)†
Platelet count (× 10^3/μL)*	135.5 ± 75.9 (11–714)‡
AST-to-platelet ratio index score*	1.50 ± 1.97 (0.1–17.4)
Fibrosis-4 score*	5.8 ± 5.8 (0.33–49.5)
Subpopulation with cirrhosis§	59
International normalized ratio*	1.23 ± 0.29 (0.8–3.2)
Serum bilirubin (mg/dL)*	1.90 ± 3.06 (0.2–34.3)‖
Serum albumin (g/dL)*	3.53 ± 0.71 (1.5–5.5)#
Serum creatinine (mg/dL)*	1.03 ± 0.52 (0.54–8.26)**
MELD score*	11.2 ± 4.7 (6.4–36.7)
Child Pugh score	
A	220 (61)
B	84 (23)
C	30 (8)

Note.—Unless otherwise indicated, data are number of patients, with percentage in parentheses. For patients who underwent multiple MR elastography examinations, data presented are at the time of the first MR imaging examination.

* Data are means ± standard deviation, with the range in parentheses.

† To convert to Système International (SI) units (microkatals per liter), multiply by 0.0167.

‡ To convert to SI units (× 10^9 per liter), multiply by 1.

§ International normalized ratio, MELD score, and Child-Pugh score were not available for 25 patients.

‖ To convert to SI units (micromoles per liter), multiply by 17.104.

To convert to SI units (grams per liter), multiply by 10.

** To convert to SI units (micromoles per liter), multiply by 88.4.

Factors of MR Elastography Failure

The results are presented in Table 2. Technical failure of MR elastography was not significantly associated with sex, age, or race and ethnicity. A higher weight and BMI were associated with failure of MR elastography, and the technical failure rate increased with BMI (BMI < 25 vs BMI ≥25, 7.9% [22 of 279] vs 12.5% [56 of 448]; P = .021) (Fig 1), while subcutaneous fat thickness, liver fat fraction, and steatosis (as a binary measure) were not associated with MR elastography failure. A weight higher than 77.1 kg and a BMI higher than 26.8 were predictors of technical failure, with sensitivity of 59.0% (46 of 78) and 64.6% (51 of 79), respectively, and specificity of 59.9% (394 of 658) and 55.6% (387 of 696), respectively.

The presence of chronic liver disease was not associated with failure of MR elastography (P = .252), while the technical failure rate was higher in examinations of patients with liver cirrhosis and was dependent on the cause of liver disease. Examinations of patients with alcoholic liver disease had a higher risk of technical failure (28.6%, 14 of 49) compared with those of the patients with nonalcoholic liver diseases. The presence of massive ascites also was associated with failure of MR elastography (Fig 2).

In the subgroup of patients with chronic liver disease, while the AST-to-platelet ratio index score was not predictive of MR elastography failure, a higher fibrosis-4 score and a lower platelet count were associated with technical failure. In the subgroup of patients with cirrhosis, MR elastography failure was significantly associated with more advanced disease, according to Child-Pugh and MELD scores.

The use of a 3.0-T system with a GRE-based MR elastography sequence was significantly associated with technical failure, while the presence of clip artifacts was not. T2* value at 1.5 T was not a significant predictor of MR elastography failure (P = .250), while T2* value at 3.0 T was a significant predictor of MR elastography failure (P < .001). For patients imaged at

Table 2

Factors Associated with Failure of MR Elastography at Univariate Analysis

Factor	Success ($n = 781$)	Failure ($n = 80$)	OR*	*P* Value
Age†	58.1 ± 12.3	59.8 ± 11	1.01 (0.99, 1.03)	.198
Sex			1.68 (1, 2.82)	.051
Male	439/498 (88.2)	59/498 (11.8)		
Female	262/283 (92.6)	21/283 (7.4)		
Race			NA (NA)	.902
White	212/234 (90.6)	22/234 (9.4)		
Nonwhite	302/337 (89.6)	35/337 (10.4)		
Unknown	187/210 (89.0)	23/210 (11.0)		
BMI†	26.4 ± 4.7	27.8 ± 4.4	1.06 (1.01, 1.11)	.012§
BMI category‡			1.43 (1.06, 1.92)	.021§
<19	18/19 (94.7)	1/19 (5.3)		
19–25	239/260 (91.9)	21/260 (8.1)		
25–30	262/295 (88.8)	33/295 (11.2)		
> 30	130/153 (85.0)	23/153 (15.0)		
Weight (kg)†	75.7 ± 15.4	81.1 ± 4.4	1.02 (1.01, 1.04)	.005§
Chronic liver disease			2.21	.001§
None	121/131 (92.4)	10/131 (7.6)		
Hepatitis C virus	311/345 (90.1)	34/345 (9.9)		
Hepatitis B virus	119/134 (88.8)	15/134 (11.2)		
Alcohol abuse	35/49 (71.4)	14/49 (28.6)		
Nonalcoholic steatohepatitis	48/52 (92.3)	4/52 (7.7)		
Others	55/56 (98.2)	1/56 (1.8)		
Miscellaneous	12/14 (85.7)	2/14 (14.3)		
Liver morphology			2.09	.004§
Noncirrhotic or indeterminate	331/355 (93.2)	24/355 (6.8)		
Cirrhosis	370/426 (86.9)	56/426 (13.1)		
Liver iron deposition#			5.17	<.001§
No iron	566/604 (93.7)	38/604 (6.3)		
Iron deposition	121/163 (74.2)	42/163 (25.8)		
T2* at 1.5 T (msec)	26.5 ± 6.8	28.4 ± 5.2		.250
T2* at 3.0 T (msec)	21.2 ± 5.7	12.9 ± 7.1		<.001§
Liver steatosis status‖			1.22 (0.75, 1.99)	.449
No steatosis	492/545 (90.3)	53/545 (9.7)		
Liver steatosis	206/233 (88.4)	27/233 (11.6)		
Fat fraction (%)†	3.3 ± 5.8	4.0 ± 6.2	1.02 (0.98, 1.06)	.241
Subcutaneous fat thickness (mm)†	12.4 ± 6.1	13.0 ± 6.7	1.01 (0.98, 1.05)	.510
Ascites			2.13 (1.71, 2.65)	<.001§
None	509/551 (92.4)	42/551 (7.6)		
Mild	136/148 (91.9)	12/148 (8.1)		
Moderate	38/41 (92.7)	3/41 (7.3)		
Massive	18/41 (43.9)	23/41 (56.1)		
Presence of metallic artifacts	218/236 (92.4)	18/236 (7.6)	0.64 (0.37, 1.11)	.113
Field strength			4.93 (2.62, 9.26)	<.001§
1.5 T	326/338 (96.4)	12/338 (3.6)		
3.0 T	375/443 (84.7)	68/443 (15.3)		
Population with chronic liver disease				
AST-to-platelet ratio index score†	1.46 ± 1.96	1.72 ± 1.53	1.06 (0.95, 1.19)	.208
Fibrosis-4 score†	5.65 ± 5.85	7.16 ± 5.14	1.04 (1, 1.07)	.022§
Platelet count†	136.61 ± 75.15	108.97 ± 136.61	0.99 (0.99, 1)	.002§

Table 2 (*continues*)

Table 2 (continued)

Factors Associated with Failure of MR Elastography at Univariate Analysis

Factor	Success (n = 781)	Failure (n = 80)	OR*	P Value
Population with cirrhosis				
Child-Pugh score**			2.57 (1.73, 3.82)	<.001§
A	243/266 (91.4)	23/266 (8.6)		
B	78/95 (82.1)	17/95 (17.9)		
C	19/32 (59.4)	13/32 (40.6)		
MELD score†**	10.7 ± 4.5	13.7 ± 5.2	1.08 (1.03, 1.13)	<.001§

Note.—Unless otherwise indicated, data are proportion of patients, with percentage in parentheses. Generalized estimating equations were based on a binary logistic regression model. NA = not available.

* Data in parentheses are 95% CIs.

† Data are means ± standard deviation.

‡ Not available for 54 patients.

§ Indicates a significant association.

Not available for 14 patients.

‖ Not available for 3 patients.

** Not available in 33 patients.

Figure 1

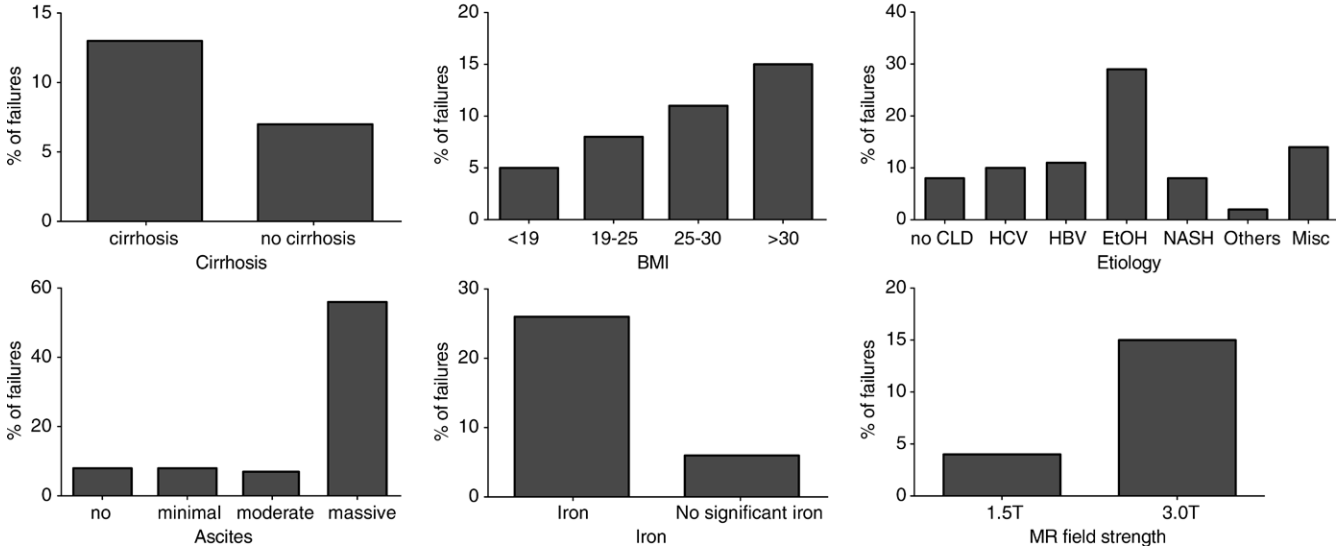

Figure 1: Graphs show distributions of the failure rate of MR elastography (acquired with two-dimensional GRE sequence) based on the presence or absence of cirrhosis, ascites, iron, MR field strength, BMI, and chronic liver disease etiology. Iron deposition is defined as liver T2* less than 24 msec at 1.5 T and less than 14 msec at 3.0 T; liver steatosis is defined as fat fraction greater than 5%. *CLD* = chronic liver disease, *EtOH* = alcohol abuse, *HBV* = hepatitis B virus, *HCV* = hepatitis C virus, *Misc* = association of multiple causes, *NASH* = nonalcoholic steatohepatitis.

3.0 T, a T2* less than or equal to 15.0 msec was predictive of failure, with sensitivity of 67.6% (46 of 68) and specificity of 87.6% (325 of 371). The presence of iron deposition (as a binary measure) was significantly associated with MR elastography failure (Fig 3). The receiver operating characteristic curve analyses for predicting failure with T2* value, weight, and BMI are presented in Figure 4 and Table 3.

Independent Factors of MR Elastography Failure

In the multivariable analysis, presence of liver iron ($P < .001$; OR, 8.88 [95% CI: 4.89, 16.15]), use of a 3.0-T system ($P < .001$; OR, 9.93 [95% CI: 4.62, 21.35]), massive ascites ($P < .001$; OR, 21.44; [95% CI: 9.28, 49.51]), and higher BMI ($P = .004$; OR, 1.09 [95% CI: 1.03,1.16]) were all independently associated with MR elastography technical failure. The use of 3.0 T, which was associated with at least two of the three other independent factors, led to

Figure 2

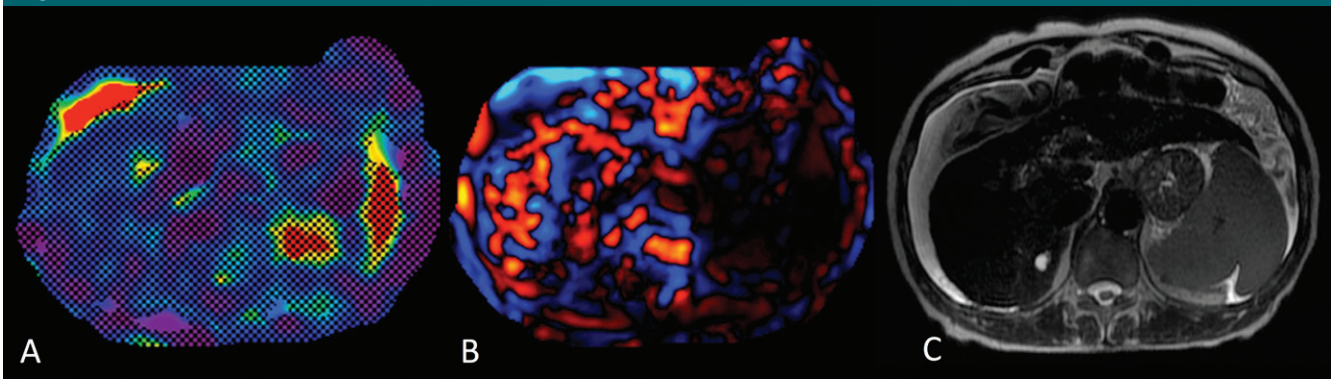

Figure 2: Images in a 62-year-old woman with alcoholic cirrhosis. *A*, MR elastogram of the liver acquired by using a two-dimensional GRE sequence shows failure, with no pixel value with a confidence index higher than 95% on the confidence map and, *B*, no wave propagation (disorganized waves) on the wave image. *C*, T2-weighted single-shot fast spin-echo image shows massive ascites. Patient had iron deposition with a T2* of 5.5 msec at 3.0 T and was not overweight (BMI = 21.8).

Figure 3

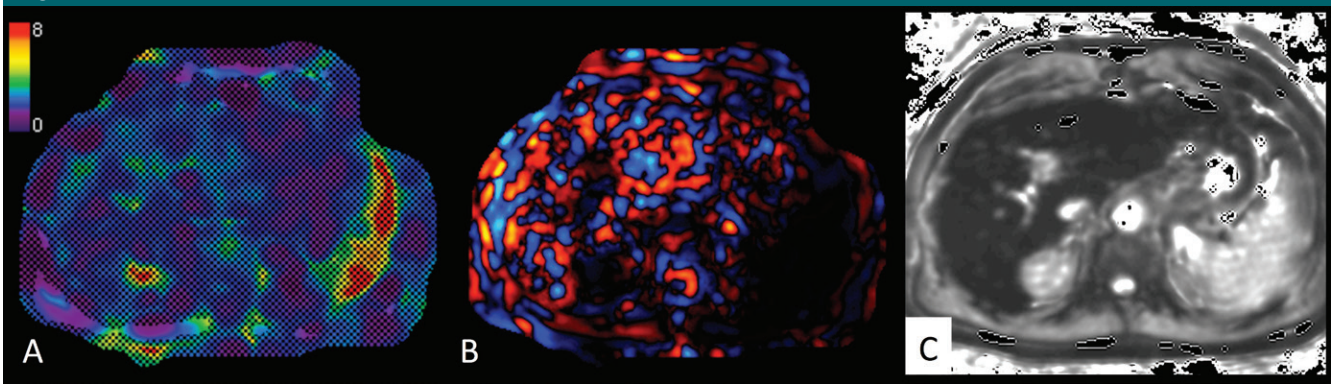

Figure 3: Images in a 61-year-old man with hepatitis C virus cirrhosis. *A*, Liver MR elastogram acquired by using two-dimensional GRE sequence shows failure, with no pixel value with a confidence index higher than 95% on the confidence map and, *B*, no wave propagation (disorganized waves) on the wave image. *C*, T2* map shows severe iron deposition with T2* of 5 msec at 3.0 T. Patient was also overweight (BMI = 28.6) with no ascites.

technical failure in 38 of 56 (67.9%) examinations (Table 4).

Failed Examinations

Details of independent factors of failure are presented in Table 4. Only two failed MR elastography examinations did not show at least one independent determinant of MR elastography failure, while all the patients with iron deposition and massive ascites and who underwent MR elastography at 3.0 T with a GRE-based sequence had failed examinations.

Patients with Repeat MR Elastography

Sixty-nine patients underwent two MR elastography examinations in our cohort. Among them, 10 had one technical failure and one had two failures. For eight (80%) of the patients with one failure, the technical failure occurred at 3.0 T with the GRE-based MR elastography sequence, while the success occurred at 1.5 T (Fig 5). For one patient, the two MR elastography examinations were performed at 3.0 T, but the T2* decreased between the two examinations, and iron deposition was present when the MR elastography failed. The last patient underwent failed MR elastography at 1.5 T but MR elastography was successful at 3.0 T. No difference was found between the two examinations (no iron deposition, massive ascites, or high BMI). The patient with the two failed MR elastography examinations was obese and the two examinations were performed at 3.0 T. Among the nine patients who underwent three MR elastography examinations, two patients had one MR elastography failure. One patient underwent three MR elastography examinations at 1.5 T, and no difference was found among the three examinations, except for borderline T2* (T2*, 23.6 msec) at one of the successful examinations. The second patient experienced technical failure at 3.0 T and success at 1.5 T and 3.0 T. This patient had iron deposition as determined on the basis of three MR imaging examinations. The patient who underwent

Figure 4

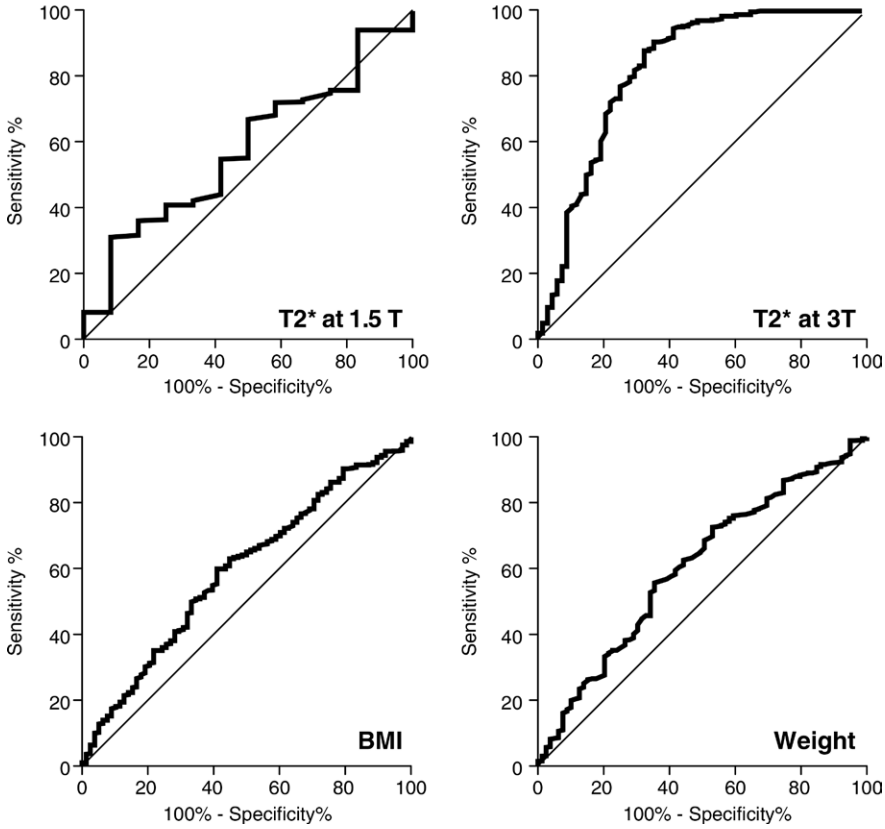

Figure 4: Graphs show receiver operating characteristic curves for prediction of failure of MR elastography with use of T2*, weight, and BMI.

Table 3

Receiver Operating Characteristic Curve Analysis for Prediction of MR Elastography Failure by Using T2*, Body Weight, and BMI

Factor	Threshold	Area under the Curve*	Sensitivity	Specificity	*P* Value
T2* at 1.5 T (msec)	<24.4	0.58 (0.43, 0.72)	11/12 (91.7)	98/316 (31.0)	.371
T2* at 3.0 T (msec)	<15.0	0.81 (0.75, 0.88)	46/68 (67.7)	325/371 (87.6)	<.0001
Weight (kg)	>77.1	0.60 (0.54, 0.67)	51/79 (64.6)	387/696 (55.6)	.003
BMI (kg/m^2)	>26.8	0.59 (0.53, 0.66)	46/78 (59.0)	394/658 (59.9)	.007

Note.—Unless otherwise indicated, data are proportion of patients, with percentage in parentheses.

* Data in parentheses are 95% CIs.

four MR elastography examinations experienced no technical failure.

Discussion

In our cohort of 781 MR elastography examinations in 691 patients, MR elastography failed in 3.5% of the 1.5-T examinations and in 15.3% of the 3.0-T examinations, when the same type of GRE-based MR elastography pulse sequence was used. Massive ascites, iron deposition, and the use of high field strength (3.0 T) were strongly associated with technical failure.

The technical failure rate of MR elastography reported in our study at 1.5 T is consistent with rates previously reported (4%–5.6%) (9,14,26). On the other hand, the technical failure rate observed at 3.0 T was considerably higher (more than four times higher) than that at 1.5 T, although it was comparable to the technical failure rate reported for transient elastography. We believe that the explanation for the higher rate of failure at 3.0 T observed in our study rests in the use of a GRE-based MR elastography pulse sequence. The susceptibility artifacts are higher at 3.0 T, approximately twice as high as those at 1.5 T (27,28), because they are responsible for signal loss and dephasing (29), which may decrease the quality of wave imaging. Accordingly, a spin-echo echo-planar imaging (EPI) pulse sequence is now being used routinely in commercial versions of MR elastography at 3.0 T (30,31). However, some clinical MR imaging systems operating at 3.0 T have not yet been modified in this regard. Recently, Yoshimitsu et al (30) reported no technical failures in a series of 70 clinical MR elastography examinations performed at 3.0 T with a spin-echo EPI sequence. Moreover, results of a recent study (21) showed that the quality of the GRE MR elastography images was lower than the quality of the spin-echo EPI MR elastography images at 3.0 T, with no failure with the use of the spin-echo EPI sequence in a cohort of 50 patients.

As expected and previously described, the presence of iron deposition is associated with technical failure of MR elastography of the liver (9,14). In Yin et al (14), 55 of the 77 (71%) cases of failure had an inadequate signal-to-noise ratio due to iron overload, and in Yoon et al (9), all six cases of failure were in patients with iron deposition at MR imaging and pathologic examination. Results of recent studies (21) have shown that the quality of the GRE MR elastography images correlated with liver T2* values at 3.0 T, with lower quality with shorter T2*, (ie, when the iron deposition increases). The long echo time of GRE MR elastography sequences explains the low signal-to-noise

Table 4

Description of the Factors Responsible for Failure of MR Elastography Examinations

Factors of Failure	Failed Examinations ($n = 80$)	Failed Examinations per Patient Factor ($n = 781$)*
3.0 T, iron deposition, massive ascites, and overweight†	4 (5.0)	4/4 (100)
3.0 T, iron deposition, massive ascites	4 (5.0)	4/4 (100)
3.0 T, iron deposition, and overweight†	21 (26.2)	21/35 (60.0)
3.0 T, massive ascites, and overweight†	9 (11.2)	9/13 (69.2)
3.0 T and iron deposition	12 (15.0)	12/31 (38.7)
3.0 T and massive ascites	2 (2.5)	2/3 (66.6)
3.0 T and overweight†	13 (16.2)	13/203 (6.4)
Iron deposition and massive ascites	1 (1.2)	1/3 (33.3)
Massive ascites and overweight†	3 (3.8)	3/7 (42.8)
3.0 T	3 (3.8)	3/147 (2.0)
Overweight†	6 (7.5)	6/146 (4.1)
None‡	2 (2.5)	2/92 (2.1)

Note.—Unless otherwise indicated, data are number of examinations, with percentage in parentheses.

* Data are proportion of the total number of patients with each factor who experienced MR elastography failure, with percentage in parentheses.

† Overweight defined as BMI > 25.

‡ None = no use of 3.0 T, no iron deposition, no massive ascites, no overweight.

Figure 5

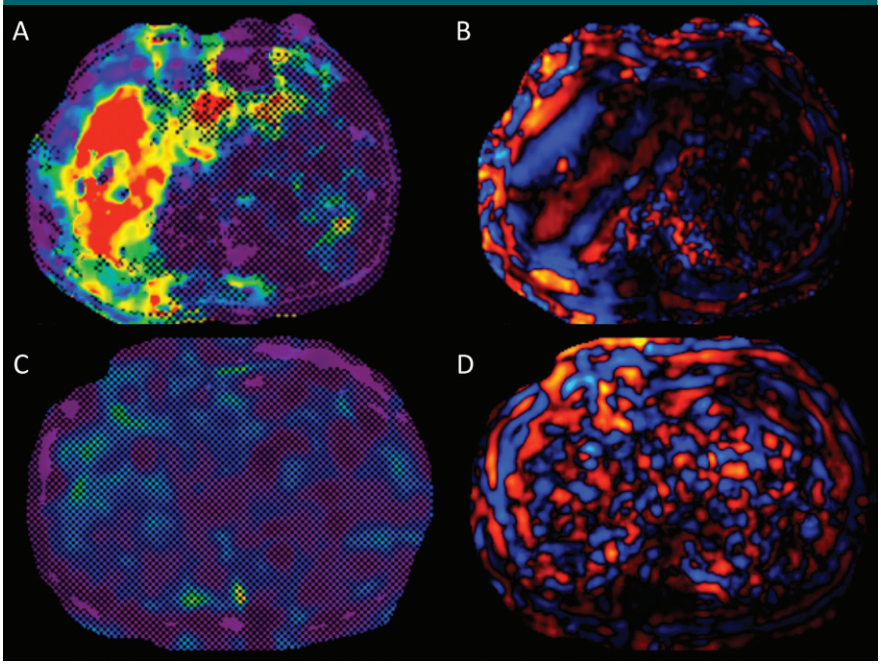

Figure 5: Images in a 53-year-old male patient with HCV cirrhosis. *A*, Liver MR elastogram acquired by using two-dimensional GRE sequence was successful at 1.5 T with large liver coverage by pixel values, with a confidence index higher than 95% on the confidence map and, *B*, good wave propagation, while, *C*, MR elastogram from repeat examination (162 days later) shows failure at 3.0 T, with no pixel value with a confidence index higher than 95% on the confidence map, and, *D*, no wave propagation (disorganized waves) on the wave image. Patient had iron deposition on images from both examinations (T2* = 7.5 msec at 3.0 T and 17.2 msec at 1.5 T) and was overweight (BMI = 26, 27.6).

ratio in liver iron overload (32). Indeed, the echo time was similar at 3.0 T to that at 1.5 T, which may explain the highest failure rate at 3.0 T. These results suggest that alternative pulse sequences, such as spin-echo EPI with a shorter echo time, should be used at 3.0 T in patients with iron overload to decrease the risk of failure. Other options include the use of a pure spin-echo sequence, which is less affected by the T2* decay, or a GRE sequence with fractional motion encoding to minimize echo time (33,34).

In our study, a high BMI was associated with an increased rate of MR elastography technical failure. This result is in contradiction with the results of the study by Yin et al (14), which did not show a difference in BMI between the successful and failed MR elastography examinations. However, the low OR of 1.09 in our study suggests that the effect is small.

Unlike Huwart et al (26), we found that massive ascites was a predictive factor of liver MR elastography failure with the highest OR. The discrepancy with the results of Huwart et al may be due to lack of patients with massive ascites in their study. Patients with advanced cirrhosis also had a high risk of MR elastography failure, as shown by the MELD and the Child-Pugh scores. This may be explained by the increased prevalence of massive ascites in patients with advanced cirrhosis.

Our study had several limitations beyond its retrospective design. First, we assessed the failure rate by using equipment from only one manufacturer (GE Healthcare). The MR elastography acquisition parameters of systems from other vendors are very similar when the same GRE sequence is used, with reported high interplatform reproducibility (35,36). Second, our study included only MR elastography examinations performed by using a GRE MR elastography sequence. We did not use alternative sequences such as the spin-echo EPI MR elastography sequence, which is now available on the 3.0-T system used in this study, or fractional GRE MR elastography (30,34). However,

the technical failure rate with the GRE MR elastography sequence at 3.0 T has not been documented specifically in the literature, to our knowledge. Third, we did not assess the reliability of the MR elastography examination, but only technical failure, and reliability is an important factor used to determine if an examination is interpretable for transient elastography, the most commonly used elastography method. However, a widely accepted criterion for reliability of MR elastography results has not yet been clearly defined in the literature, to our knowledge. Yoon et al (9), by using a definition similar to that for transient elastography or shear-wave elastography and a median and interquartile range liver stiffness ratio of greater than 30%, found that no patients had unreliable liver stiffness measurements. Fourth, we evaluated the fat fraction by using the two-point Dixon method and not a multiecho Dixon method with measurement of proton density fat fraction, which is more accurate (23). However, results of previous studies (37,38) have shown that liver fat does not seem to affect liver stiffness measurements with MR elastography.

In conclusion, our results confirmed that at 1.5 T, the technical failure rate of MR elastography is low, similar to that reported in other studies. Our evaluation of the performance of a GRE-based MR elastography pulse sequence at 3.0 T demonstrated that the technical failure rate was substantially higher, indicating the critical importance of using an alternative pulse sequence such as spin-echo EPI or fractional GRE pulse sequences. Massive ascites, iron deposition, and high BMI were additional independent factors associated with failure of MR elastography of the liver with a two-dimensional GRE pulse sequence.

Disclosures of Conflicts of Interest: M.W. disclosed no relevant relationships. **I.C.S.** disclosed no relevant relationships. **G.L.** Activities related to the present article: disclosed no relevant relationships. Activities not related to the present article: employed by Mount Sinai Hospital. Other relationships: disclosed no relevant relationships. **S.E.** disclosed no relevant relationships. **J.L.** disclosed no relevant relationships. **C.B.** disclosed no relevant relationships. **N.C.** disclosed no relevant relationships. **G.A.** disclosed no relevant relationships. **M.F.** Activities related to the present article: disclosed no relevant relationships. Activities not related to the present article: employment with and stock options from GE Healthcare. Other relationships: disclosed no relevant relationships. **J.S.B.** disclosed no relevant relationships. **R.L.E.** Activities related to the present article: loan of fibroscan device for study from Echosens, author and the Mayo Clinic have intellectual property rights and financial interest in MR elastography technology. Activities not related to the present article: uncompensated CEO of Resoundant, royalties and stock/stock options from Resoundant. **B.T.** Activities related to the present article: disclosed no relevant relationships. Activities not related to the present article: grants from Guerbet. Other relationships: disclosed no relevant relationships.

References

1. Bravo AA, Sheth SG, Chopra S. Liver biopsy. N Engl J Med 2001;344(7):495–500.
2. Bedossa P, Dargère D, Paradis V. Sampling variability of liver fibrosis in chronic hepatitis C. Hepatology 2003;38(6):1449–1457.
3. Castera L, Bedossa P. How to assess liver fibrosis in chronic hepatitis C: serum markers or transient elastography vs. liver biopsy? Liver Int 2011;31(Suppl 1):13–17.
4. Friedrich-Rust M, Ong MF, Martens S, et al. Performance of transient elastography for the staging of liver fibrosis: a meta-analysis. Gastroenterology 2008;134(4):960–974.
5. Castéra L, Foucher J, Bernard PH, et al. Pitfalls of liver stiffness measurement: a 5-year prospective study of 13,369 examinations. Hepatology 2010;51(3):828–835.
6. Ferraioli G, Tinelli C, Dal Bello B, et al. Accuracy of real-time shear wave elastography for assessing liver fibrosis in chronic hepatitis C: a pilot study. Hepatology 2012;56(6):2125–2133.
7. Friedrich-Rust M, Nierhoff J, Lupsor M, et al. Performance of Acoustic Radiation Force Impulse imaging for the staging of liver fibrosis: a pooled meta-analysis. J Viral Hepat 2012;19(2):e212–e219.
8. Bota S, Sporea I, Sirli R, et al. Factors associated with the impossibility to obtain reliable liver stiffness measurements by means of Acoustic Radiation Force Impulse (ARFI) elastography--analysis of a cohort of 1,031 subjects. Eur J Radiol 2014;83(2):268–272.
9. Yoon JH, Lee JM, Joo I, et al. Hepatic fibrosis: prospective comparison of MR elastography and US shear-wave elastography for evaluation. Radiology 2014;273(3):772–782.
10. Dyvorne HA, Jajamovich GH, Bane O, et al. Prospective comparison of magnetic resonance imaging to transient elastography and serum markers for liver fibrosis detection. Liver Int 2016;36(5):659–666.
11. Huwart L, Sempoux C, Salameh N, et al. Liver fibrosis: noninvasive assessment with MR elastography versus aspartate aminotransferase-to-platelet ratio index. Radiology 2007;245(2):458–466.
12. Venkatesh SK, Wang G, Lim SG, Wee A. Magnetic resonance elastography for the detection and staging of liver fibrosis in chronic hepatitis B. Eur Radiol 2014;24(1):70–78.
13. Imajo K, Kessoku T, Honda Y, et al. Magnetic resonance imaging more accurately classifies steatosis and fibrosis in patients with nonalcoholic fatty liver disease than transient elastography. Gastroenterology 2016;150(3):626–637.e7.
14. Yin M, Glaser KJ, Talwalkar JA, Chen J, Manduca A, Ehman RL. Hepatic MR elastography: clinical performance in a series of 1377 consecutive examinations. Radiology 2016;278(1):114–124.
15. Sterling RK, Lissen E, Clumeck N, et al. Development of a simple noninvasive index to predict significant fibrosis in patients with HIV/HCV coinfection. Hepatology 2006;43(6):1317–1325.
16. Kamath PS, Wiesner RH, Malinchoc M, et al. A model to predict survival in patients with end-stage liver disease. Hepatology 2001;33(2):464–470.
17. Pugh RN, Murray-Lyon IM, Dawson JL, Pietroni MC, Williams R. Transection of the oesophagus for bleeding oesophageal varices. Br J Surg 1973;60(8):646–649.
18. Motosugi U, Ichikawa T, Sou H, et al. Effects of gadoxetic acid on liver elasticity measurement by using magnetic resonance elastography. Magn Reson Imaging 2012;30(1):128–132.
19. Manduca A, Oliphant TE, Dresner MA, et al. Magnetic resonance elastography: noninvasive mapping of tissue elasticity. Med Image Anal 2001;5(4):237–254.
20. Silva AM, Grimm RC, Glaser KJ, et al. Magnetic resonance elastography: evaluation of new inversion algorithm and quantitative analysis method. Abdom Imaging 2015;40(4):810–817.
21. Wagner M, Besa C, Bou Ayache J, et al. Magnetic resonance elastography of the liver: qualitative and quantitative comparison of gradient echo and spin echo echoplanar imaging sequences. Invest Radiol 2016;51(9):575–581.
22. Awaya H, Mitchell DG, Kamishima T, Holland G, Ito K, Matsumoto T. Cirrhosis: modified caudate-right lobe ratio. Radiology 2002;224(3):769–774.

23. Reeder SB, Cruite I, Hamilton G, Sirlin CB. Quantitative assessment of liver fat with magnetic resonance imaging and spectroscopy. J Magn Reson Imaging 2011;34(4):729–749.

24. Hernando D, Qazi N, Reeder S. Calibration of confounder-corrected R2* for liver iron quantification at 1.5T and 3T: preliminary results [abstr]. In: Proceedings of the Twenty-First Meeting of the International Society for Magnetic Resonance in Medicine. Berkeley, Calif: International Society for Magnetic Resonance in Medicine, 2013.

25. Storey P, Thompson AA, Carqueville CL, Wood JC, de Freitas RA, Rigsby CK. R2* imaging of transfusional iron burden at 3T and comparison with 1.5T. J Magn Reson Imaging 2007;25(3):540–547.

26. Huwart L, Sempoux C, Vicaut E, et al. Magnetic resonance elastography for the noninvasive staging of liver fibrosis. Gastroenterology 2008;135(1):32–40.

27. Bernstein MA, Huston J 3rd, Ward HA. Imaging artifacts at 3.0T. J Magn Reson Imaging 2006;24(4):735–746.

28. Graf H, Lauer UA, Berger A, Schick F. RF artifacts caused by metallic implants or instruments which get more prominent at 3 T: an in vitro study. Magn Reson Imaging 2005;23(3):493–499.

29. Merkle EM, Dale BM, Thomas J, Paulson EK. MR liver imaging and cholangiography in the presence of surgical metallic clips at 1.5 and 3 Tesla. Eur Radiol 2006;16(10):2309–2316.

30. Yoshimitsu K, Mitsufuji T, Shinagawa Y, et al. MR elastography of the liver at 3.0 T in diagnosing liver fibrosis grades; preliminary clinical experience. Eur Radiol 2016;26(3):656–663.

31. Bohte AE, de Niet A, Jansen L, et al. Noninvasive evaluation of liver fibrosis: a comparison of ultrasound-based transient elastography and MR elastography in patients with viral hepatitis B and C. Eur Radiol 2014;24(3):638–648.

32. Positano V, Salani B, Pepe A, et al. Improved T2* assessment in liver iron overload by magnetic resonance imaging. Magn Reson Imaging 2009;27(2):188–197.

33. Huwart L, Salameh N, ter Beek L, et al. MR elastography of liver fibrosis: preliminary results comparing spin-echo and echo-planar imaging. Eur Radiol 2008;18(11):2535–2541.

34. Garteiser P, Sahebjavaher RS, Ter Beek LC, et al. Rapid acquisition of multifrequency, multislice and multidirectional MR elastography data with a fractionally encoded gradient echo sequence. NMR Biomed 2013;26(10):1326–1335.

35. Serai SD, Yin M, Wang H, Ehman RL, Podberesky DJ. Cross-vendor validation of liver magnetic resonance elastography. Abdom Imaging 2015;40(4):789–794.

36. Yasar TK, Wagner M, Bane O, et al. Interplatform reproducibility of liver and spleen stiffness measured with MR elastography. J Magn Reson Imaging 2016;43(5):1064–1072.

37. Salameh N, Larrat B, Abarca-Quinones J, et al. Early detection of steatohepatitis in fatty rat liver by using MR elastography. Radiology 2009;253(1):90–97.

38. Shi Y, Guo Q, Xia F, et al. MR elastography for the assessment of hepatic fibrosis in patients with chronic hepatitis B infection: does histologic necroinflammation influence the measurement of hepatic stiffness? Radiology 2014;273(1):88–98.